C. R. Mecanique 346 (2018) 532–538

Contents lists available at ScienceDirect

Comptes Rendus Mecanique

www.sciencedirect.com

Model reduction, data-based and advanced discretization in computational mechanics

Diffuse manifold learning of the geometry of woven reinforcements in composites

Anna Madra [a,*], Piotr Breitkopf [b], Balaji Raghavan [c], François Trochu [d]

[a] Department of Aeronautics and Astronautics, Massachusetts Institute of Technology, Cambridge, MA 02139, USA
[b] Laboratoire Roberval, UMR 7337, UTC–CNRS, Université de technologie de Compiègne, Centre de recherches de Royallieu, CS 60319, 60203 Compiègne cedex, France
[c] Laboratoire de génie civil et génie mécanique, EA 3913, INSA Rennes, 35708 Rennes, France
[d] Chair on Composites of High Performance (CCHP), Mechanical Engineering Department, Center of Research on Polymers and Composites (CREPEC), École polytechnique de Montréal, Montréal H3C 3A7, Canada

ARTICLE INFO

Article history:
Received 16 November 2017
Accepted 21 March 2018
Available online 27 April 2018

Keywords:
Model reduction
Diffuse Approximation
Composites
X-ray microtomography

ABSTRACT

When attempting to build mesoscale geometric models of woven reinforcements in composites based on X-ray microtomography data, we frequently run into ambiguous situations due to noise, particularly in contact zones between fiber tows, resulting in inadmissible cross-sectional shapes. We propose here a custom-built shape-manifold approach based on kernel PCA, *k*-means classification and Diffuse Approximation to identify, "repair" such badly segmented shapes in the feature space, and finally recover admissible shapes in the original space.

1. Introduction

In the field of aeronautics, and increasingly in the automobile sector, composites with woven reinforcements are the material of choice for high-performance applications. 3D volume imaging techniques such as X-ray microtomography provide detailed information on the geometry of the material at the micro- and mesoscales. Geometrical reconstruction based on microtomographic scans gives us an opportunity to create realistic numerical models suitable for finite element simulation of the manufacturing processes involved or for identifying the mechanical properties of the material by homogenization.

However, several challenges emerge while creating such geometric reconstructions. Firstly, the microtomographic scans need to be segmented, i.e. the elements corresponding to particular fiber tows composing the woven architecture must be identified, e.g., by determining the contours of the tow cross-sections on consecutive 2D slices of the scan. This process may be performed manually [1], by analyzing directional gradients [2] or using learning algorithms [3]. The manual approach is clearly impractical, since a single scan is composed of thousands of slices that would each require individual treatment. On the other hand, automated segmentation may yield a possibly oversimplified geometry as in the case of gradients, or mostly well-segmented, detailed contours with a certain percentage of outliers, as is the case of the learning algorithm approach [4].

In this paper, we propose tackling the issue of outlier fiber tow contours that are incorrectly segmented by using a learning strategy [3]. We begin by projecting the level-set contour snapshots of individual contours onto the feature space

* Corresponding author.
E-mail address: amadra@mit.edu (A. Madra).

https://doi.org/10.1016/j.crme.2018.04.008
1631-0721/

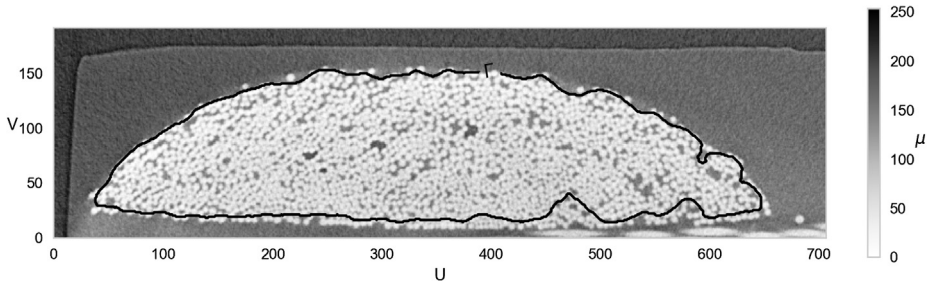

Fig. 1. 2D slice of an X-ray microtomogram with indicated contour Γ of the segmented fiber tow, grayscale values correspond to the value of X-ray attenuation coefficient μ; a plausible fiber tow contour is indicated by the black line.

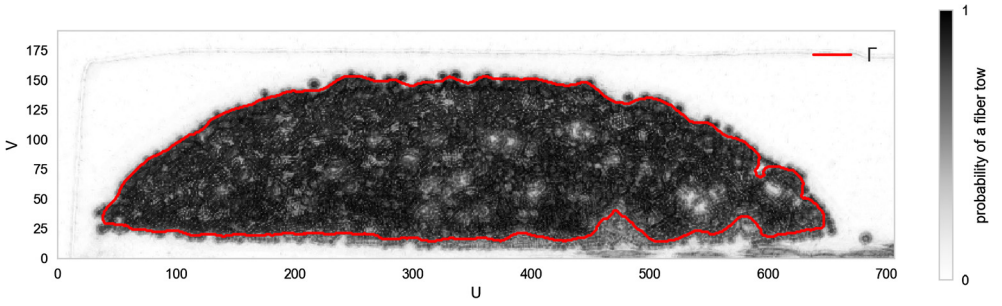

Fig. 2. Segmentation result, grayscale values correspond to the probability of tow detection. Properly identified, *regular* fiber tow section in red.

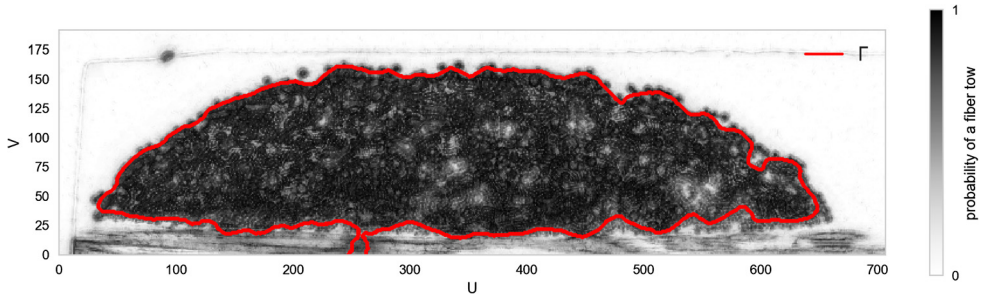

Fig. 3. Incorrectly detected, *outlier* fiber tow contour (red line); note the segmentation error zone at $U = 260, V = 0$.

using kernel-PCA [5], followed by classification using a k-means algorithm. The clusters of outliers are then identified based on an *ad hoc* criterion (e.g., failure to preserve the volume of individual fibers) and are then removed from the snapshot base which is *once again* decomposed using kernel-PCA. The shape manifold(s) of the admissible contours is/are then described by using Diffuse Approximation in the feature space. A "repaired" outlier is then hypothesized as the closest point on the manifold of admissible shapes and is obtained in the form of a set of diffuse weights with respect to neighboring admissible shapes. Finally, these weights allow us to solve the pre-image problem, i.e. finding the actual shape of the "repaired" fiber tow section in the *original* observation space.

2. Contour representation in feature space

Consider a series of contours $\Gamma^{(i)}$, $i = 1, \ldots, N_t$ of a fiber tow cross-section obtained by structure segmentation using learning algorithms of N_t subsequent 2D slices of a tomogram. A sample contour is shown in Fig. 1.

The number of individual fibers in a fiber tow is considered constant and post-processing of the image gives us the first information as to whether a given section may be considered as a *regular* one (Fig. 2), exhibiting an admissible variability due to the measurement error (which can be further taken into account for example, by introducing the "nugget effect" in kriging approximation [3]) or it must be classified as an *outlier* (Fig. 3) requiring special treatment like the one presented in the present work.

Each contour, regular or outlier, simply or multiply connected, may be represented as the zero level set of a level set function ϕ [6] defined within the whole image slice such that

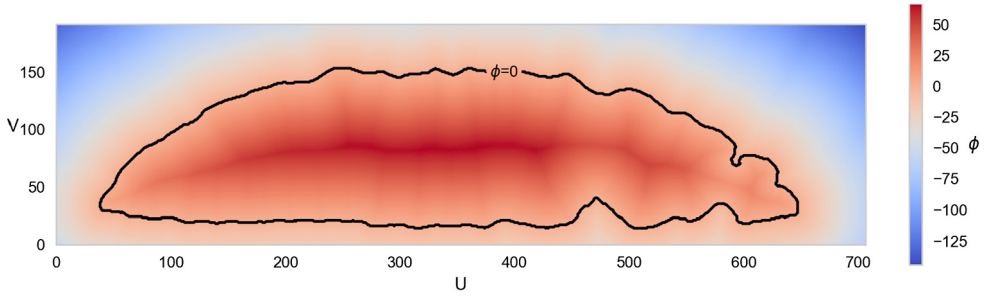

Fig. 4. An example of a level set snapshot s of a regular tow contour with $\phi = 0$ in black.

$$\begin{cases} \phi > 0, \text{ if inside the curve} \\ \phi < 0, \text{ if outside the curve} \end{cases} \tag{1}$$

as illustrated in (Fig. 4). The signed distance function meets the requirements for ϕ, and has been chosen in the present work since it may be efficiently computed from the discrete contour representation.

The Eulerian representation of the fiber tow is then given in the form of a set S of N_t snapshots $s^{(i)}$ of ϕ evolving within a fixed $N_x \times N_y$ grid (Fig. 4)

$$s^{(i)} \in \mathbb{R}^D, \quad i = 1, \ldots, N_t, \quad D = N_x \times N_y \tag{2}$$

considered centered and normalized without loss of generality.

3. Kernel PCA

The feature space F equipped with the dot product defined by the kernel function $k(.,.)$ is introduced by the mapping

$$\varphi : \mathbb{R}^D \to F \tag{3}$$

yielding the set of snapshot images $\Phi = [\varphi(s^{(1)}), \ldots, \varphi(s^{(N_t)})]$, which is subjected to re-centering in F by means of the matrix H

$$H = I - \frac{1}{N_t} \mathbb{1}\mathbb{1}^\intercal, \quad \mathbb{1} = \begin{bmatrix} 1 \\ \vdots \\ 1 \end{bmatrix} \tag{4}$$

yielding

$$\widetilde{\Phi} = \Phi H \tag{5}$$

The kernel PCA basis $V = [v_1, \ldots, v_{N_t}]$ in F is given by eigenvectors of

$$CV = V\Lambda_c \tag{6}$$

with covariance matrix C

$$C = \widetilde{\Phi}\widetilde{\Phi}^\intercal \tag{7}$$

This problem being intractable due to the dimensions of F, we consider the smaller eigenproblem $\widetilde{\Phi}^\intercal\widetilde{\Phi}$ of dimension $N_t \times N_t$

$$H^\intercal K H = U\Lambda \tag{8}$$

with

$$K = \Phi^\intercal\Phi, \quad K_{ij} = k(s^{(i)}, s^{(j)}) \tag{9}$$

The eigenvalues Λ of (8) are equal to the first m non-zero eigenvalues Λ_c and decrease rapidly, such that a low number of modes is sufficient to get an approximation of the snapshots to a required precision. A typical evolution of the Frobenius norm of the snapshot matrix reconstruction error is shown in Fig. 5.

By performing Singular Value Decomposition of $\widetilde{\Phi}$, it may be shown that the desired basis vectors V are given by

$$V = \widetilde{\Phi}U\Lambda^{-1} \tag{10}$$

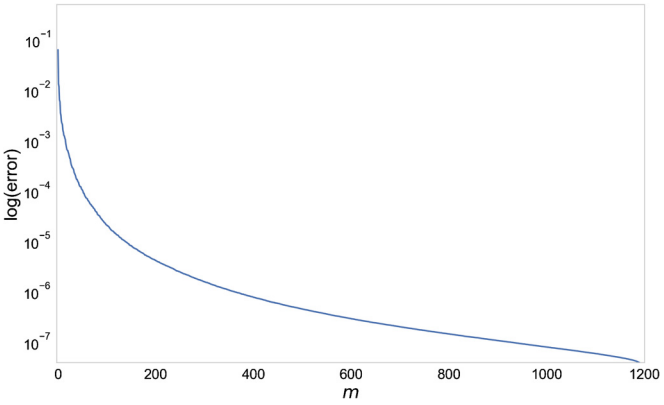

Fig. 5. Evolution of Frobenius norm of snapshot matrix reconstruction error $\varepsilon = \frac{\sum_{i=m+1}^{N_t} \lambda_i}{\sum_{j=1}^{N_t} \lambda_j}$ with increasing number of eigenvectors for 1200 successive cross sections of the fiber tow.

The coordinates of s in F are then obtained by projecting $\varphi(s)$ on V

$$A = [s^{(i)}, \ldots, s^{(N_t)}]^{\mathsf{T}} V = K V \Lambda^{-1} \tag{11}$$

with

$$A = \begin{bmatrix} \mathbb{\alpha}^{(1)T} \\ \vdots \\ \mathbb{\alpha}^{(N_t)T} \end{bmatrix}, \quad \mathbb{\alpha}^{(i)} = \begin{bmatrix} \alpha_1^{(i)} \\ \vdots \\ \alpha_{N_t}^{(i)} \end{bmatrix}, \quad i = 1, \ldots, N_t \tag{12}$$

and require (as was the case for the computation of V) only the evaluations of kernel function $k(.,.)$; in other words, they do not require the use or even knowledge of the explicit form of the mapping $\varphi(.)$ during the entire process.

4. Clustering

K-means clustering [4] is performed in F, based on the L_2 norm distance

$$\begin{aligned} \text{dist}(\varphi(s^{(i)}), \varphi(s^{(j)})) &= (\varphi(s^{(i)}) - \varphi(s^{(j)}))^{\mathsf{T}} (\varphi(s^{(i)}) - \varphi(s^{(j)})) \\ &= k(s^{(i)}, s^{(i)}) + k(s^{(j)}, s^{(j)}) - 2k(s^{(i)}, s^{(j)}) \end{aligned} \tag{13}$$

computed again by using the kernel $k(.,.)$ alone.

Fig. 6, obtained for a complete set of $N_t = 1200$ consecutive contours of a fiber tow and a linear kernel $k(x, y) = x^{\mathsf{T}} y$, reveals two well-separated clusters, A and B. By inspection, we observe that cluster B contains a small number of outlier cross sections and may consequently be labeled as "inadmissible", while the cluster A (corresponding to the majority of regular cross sections) may be labeled as "admissible". The labeling operation may be further automated, using a variety of criteria such as the preservation of the number of individual fibers in a tow as per the manufacturer's specifications, by prescribing limits on the fiber tow cross section area/perimeter or simply the size of the clusters.

5. Diffuse manifold learning

Our approach differs from the reduced-basis PCA [7,8] and kernel PCA [9] approaches, where model reduction is accomplished by retaining basis vectors $v_1, \ldots, v_d$ corresponding to the first few eigenvalues of (8), sorted in decreasing order. Instead of truncating the basis, we postulate that the set of admissible shapes belonging to cluster A in Fig. 6 may be approximated by a smooth manifold with intrinsic dimensionality d, embedded in $\mathbb{R}^D$, with $d << D$

$$\mathcal{M}(\mathbb{\alpha}) = 0 \tag{14}$$

NOTE: High-order modes are still discarded, but merely in order to filter out noise rather than as part of the model reduction.

We observe [10] that the shape manifold, given above in an implicit form, may be approximated in a parametric manner in terms of the consecutive projection coefficients $\alpha_2 = \alpha_2(\alpha_1), \alpha_3 = \alpha_3(\alpha_1, \alpha_2), \ldots$

$$\alpha_k = \alpha_k(\alpha_1, \ldots, \alpha_{k-1}), \quad k = 2, \ldots, N_t \tag{15}$$

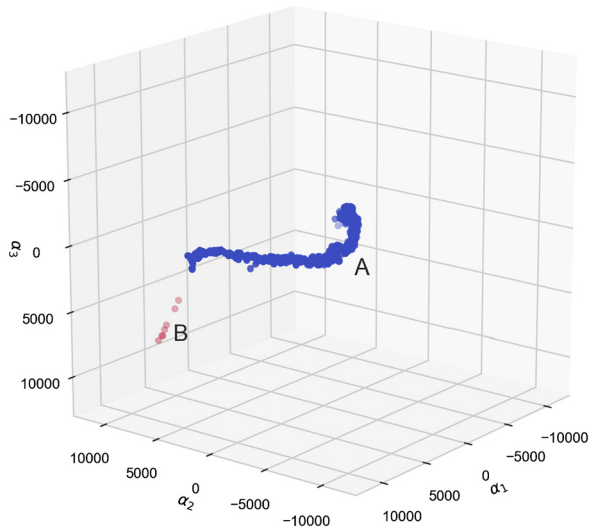

Fig. 6. Points corresponding to $N_t = 1200$ snapshots cast into the reduced feature space. Two clusters of points are indicated: A (blue dots) corresponding to correct segmentation; B (red dots) representing badly segmented outliers.

by applying Diffuse Approximation in recurrent fashion

$$\alpha_k = p^{\mathsf{T}}(\alpha_1, \ldots, \alpha_{k-1})a(\alpha_1, \ldots, \alpha_{k-1}), k = 2, \ldots, N_t \tag{16}$$

with the coefficients a obtained by minimization according to the weighted moving least squares criterion [11]

$$J(a(\mathbb{\alpha})) = \frac{1}{2} \sum_{\mathbb{\alpha}_i \in V(\mathbb{\alpha})} w(\mathbb{\alpha}^{(i)}, \mathbb{\alpha})(P^{\mathsf{T}}(\mathbb{\alpha}^{(i)})a - \mathbb{\alpha}_k^{(i)})^2 \tag{17}$$

where the neighborhood $V(\mathbb{\alpha})$ is determined by the weighting function and the radius of influence $R^{(i)}$ associated with a point α^i.

In the present work, for numerical convenience, Gaussian weighting

$$w(\alpha^{(i)}, \alpha) = \exp(-||\alpha^{(i)} - \alpha||/2R^{(i)}) \tag{18}$$

even if non-zero over the entire domain, is computed for the nearest neighbors chosen according to the criterion given in [12].

Fig. 7 shows the resulting approximation of the manifold hypersurface $\mathcal{M}_A$ obtained for the non-centered (Fig. 7a) and centered (Fig. 7b) snapshots of the cluster A (admissible shapes in Fig. 6) in the α-subspace determined by the first three coordinates $(\alpha_1^{(i)}, \alpha_2^{(i)}, \alpha_3^{(i)})$. The projection of the outlier cluster B is also indicated. It can be observed that, although outlier detection is not heavily influenced by snapshot centering, the manifold approximation is more accurate after centering.

6. Outlier repair

For an outlier snapshot $s^{(i)}$, we consider the hypothesis that a plausible "repaired" reconstruction will correspond to the closest point on $\mathcal{M}_A$ in the feature space

$$\alpha^\star = \text{Argmin}(\text{dist}(\mathcal{M}_A, \alpha^{(i)})) \tag{19}$$

This problem is solved by using the manifold walking predictor–corrector algorithm introduced by [13] and results in a feasible solution $\alpha^\star$ in F associated with the set of weights $w(\alpha^{(i)}, \alpha^\star), \alpha^i \in V(\alpha^\star)$.

In order to achieve the process of snapshot repair, we need to solve the *preimage problem* [9], which consists of snapshot reconstruction in the original space. This is done by applying the weights $w(\alpha^{(i)}, \alpha^\star)$ to the level set function snapshots in the observation space

$$s^\star = \sum_{\alpha^i \in V(\alpha^\star)} w(\alpha^{(i)}, \alpha^\star)s^{(i)} \tag{20}$$

The final reconstructed meso-structure, composed of zero-value level sets of successive cross sections of the fiber tow, is shown in Fig. 8.

The proposed approach is then integrated into the process of dual kriging reconstruction of the Representative Volume Element (RVE) of the woven composite material reinforcement [3].

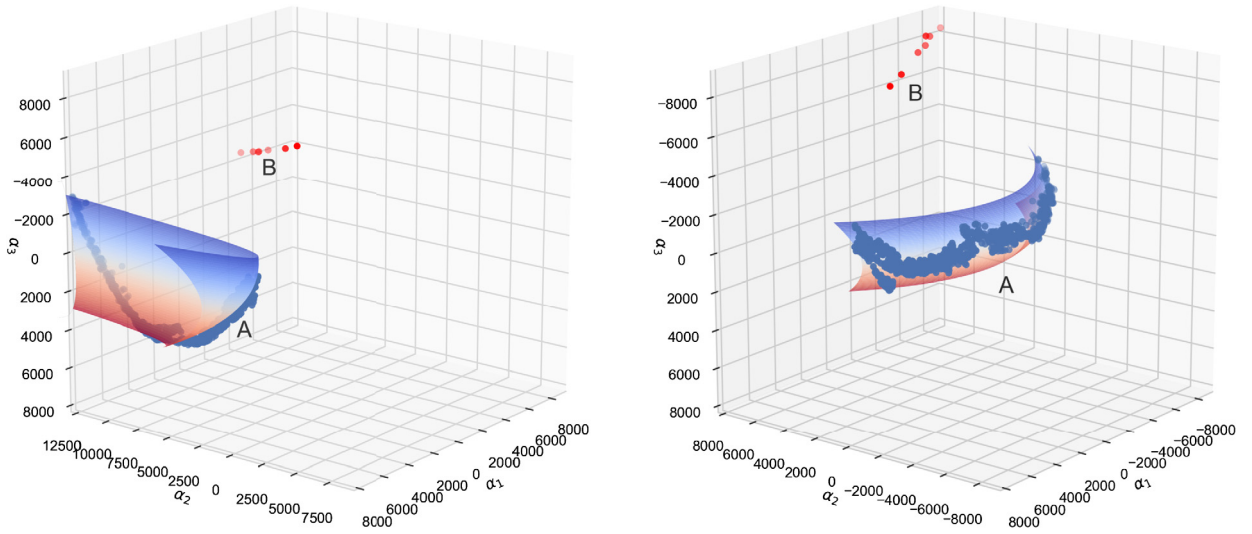

(a) Non-centered snapshots (b) Centered snapshots

Fig. 7. Points corresponding to (a) non-centered, (b) centered snapshots cast into feature space determined from the set of correctly segmented snapshots S'. A diffuse manifold fitted to the points is also shown.

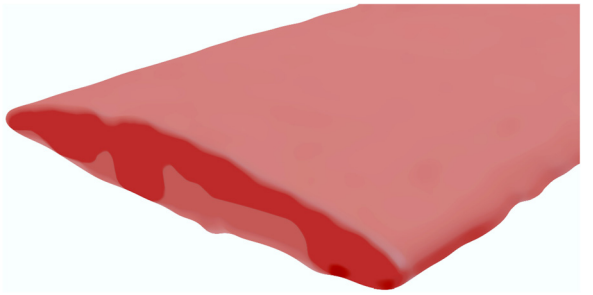

Fig. 8. The reconstructed, corrected fiber tow geometry.

7. Summary and perspectives

We have proposed here a first attempt to "repair" incorrectly segmented images of woven reinforcements in composites. The approach, based on the diffuse manifold learning technique, may be further enhanced by taking into account the position of the outliers along the axis of the tow. This may be implemented in the neighbor search for Diffuse Approximation, potentially yielding a faster algorithm and better smoothing. We have tested our approach on data for a single tow. However, in presence of multiple tows, the contact between neighboring tows must also be taken into account. Additional work is also needed to optimize the kernel function choice and for tuning the hyperparameters.

Notably, and from a hierarchical standpoint, the current work is the first and only (at this point) effort to perform manifold learning in PCA coefficient space by projecting an *experimental* target (i.e. poorly segmented) tow contour onto a basis calculated using *purely experimental* tow contour snapshots, previous efforts having focused on the first (numerical target and numerical snapshots as in [14]) and second (experimental target but numerical snapshots [15]) levels. By using numerical snapshots, we would have avoided the noise so as to more easily discover the intrinsic dimensionality, but this would have defeated the purpose of the geometry learning undertaken in the first place.

From a numerical standpoint, the main originality of the approach in the paper is the *combination* of the kPCA with the Diffuse Approximation for the first time ever.

The obvious extension of this work is by assuming Gaussian noise and kriging to describe the data, to supplement the diffuse approximation used in this work. Another effort is underway to improve data preprocessing, such as contour centering and re-orientation, which may introduce additional modes, especially for larger-scale reconstructions.

References

[1] A. Vanaerschot, F. Panerai, A. Cassell, S.V. Lomov, D. Vandepitte, N.N. Mansour, Stochastic characterisation methodology for 3-D textiles based on micro-tomography, Compos. Struct. 173 (2017) 44–52, https://doi.org/10.1016/j.compstruct.2017.03.107.

[2] I. Straumit, S.V. Lomov, M. Wevers, Quantification of the internal structure and automatic generation of voxel models of textile composites from X-ray computed tomography data, Composites, Part A, Appl. Sci. Manuf. 69 (2015) 150–158, https://doi.org/10.1016/j.compositesa.2014.11.016.
[3] A. Madra, P. Breitkopf, A. Rassineux, F. Trochu, Image-based model reconstruction and meshing of woven reinforcements in composites, Int. J. Numer. Methods Eng. 112 (9) (2017) 1235–1252, https://doi.org/10.1002/nme.5555.
[4] T. Kanungo, D. Mount, N. Netanyahu, C. Piatko, R. Silverman, A. Wu, An efficient k-means clustering algorithm: analysis and implementation, IEEE Trans. Pattern Anal. Mach. Intell. 24 (7) (2002) 881–892, https://doi.org/10.1109/TPAMI.2002.1017616, arXiv:0711.0189v1.
[5] D. Gonzalez, J.V. Aguado, E. Cueto, E. Abisset-Chavanne, F. Chinesta, kPCA-based parametric solutions within the PGD framework, Arch. Comput. Methods Eng. 25 (1) (2018) 69–86, https://doi.org/10.1007/s11831-016-9173-4.
[6] S. Osher, R. Fedkiw, Level Set Methods and Dynamic Implicit Surfaces, Springer, New York, 2003.
[7] K. Pearson, On lines and planes of closest fit to systems of points in space, Philos. Mag. 2 (6) (1901) 559–572.
[8] B. Raghavan, M. Hamdaoui, M. Xiao, P. Breitkopf, P. Villon, A bi-level meta-modeling approach for structural optimization using modified pod bases and diffuse approximation, Comput. Struct. 127 (2013) 19–28, https://doi.org/10.1016/j.compstruc.2012.06.008.
[9] B. Schölkopf, A. Smola, K.-R. Müller, Nonlinear component analysis as a kernel eigenvalue problem, Neural Comput. 10 (1998) 1299–1319.
[10] L. Xia, B. Raghavan, P. Breitkopf, W. Zhang, Numerical material representation using proper orthogonal decomposition and diffuse approximation, Appl. Comput. Math. 224 (2013) 450–462, https://doi.org/10.1016/j.amc.2013.08.052.
[11] B. Nayroles, G. Touzot, P. Villon, Generalizing the finite element method: diffuse approximation and diffuse elements, Comput. Mech. 10 (1992) 307–318.
[12] P. Breitkopf, A. Rassineux, G. Touzot, P. Villon, Explicit form and efficient computation of MLS shape functions and their derivatives, Int. J. Numer. Methods Eng. 48 (3) (2000) 451–466, https://doi.org/10.1002/(SICI)1097-0207(20000530)48:3<451::AID-NME892>3.0.CO;2-1.
[13] B. Raghavan, L. Xia, P. Breitkopf, A. Rassineux, P. Villon, Towards simultaneous reduction of both input and output spaces for interactive simulation-based structural design, Comput. Methods Appl. Mech. Eng. 265 (2013) 174–185, https://doi.org/10.1016/j.cma.2013.06.010.
[14] B. Raghavan, M. Xiao, P. Breitkopf, P. Villon, Implicit constraint handling for shape optimisation with pod-morphing, Eur. J. Comput. Mech. 21 (3–6) (2012) 325–336, https://doi.org/10.1080/17797179.2012.719316.
[15] L. Meng, B. Raghavan, O. Bartier, X. Hernot, G. Mauvoisin, P. Breitkopf, An objective meta-modeling approach for indentation-based material characterization, Mech. Mater. 107 (2017) 31–44, https://doi.org/10.1016/j.mechmat.2017.01.011.